Resonant impedances in the SPS.

T.P.R. Linnecar, E.N.Shaposhnikova

CERN, Geneva, Switzerland

1 Introduction

To prepare the SPS for the high intensity LHC beam it is important to refine the knowledge of the machine impedance. Recent measurements with beam in the SPS [1], have allowed the dominant resonant impedances seen by the beam to be found over a wide frequency range. In this paper we attempt to gather together in one place all the hardware knowledge concerning the resonant impedance of the various elements in the SPS. In this way we hope that the sources of these different impedances as measured can be identified. We have concentrated for the moment mainly on longitudinal modes as these seem to be most critical for the LHC beam in the SPS. However information is available on the transverse modes in the RF cavities and so we present this data in a separate section. The information, gleaned from many sources, is summarised in a series of tables.

2 Longitudinal modes

2.1 RF cavities

We start with the better known impedances of the six RF systems installed in the SPS. Table 1 gives the characteristics of the different modes in these cavities, ordered in ascending frequency. Table 2 shows when the cavities were installed in the machine, giving the status each year.

For each resonance we give, where possible, the following information:

1) The resonator frequency, f_{res}.

2) The source:

In Table 1 "F" indicates the fundamental mode, "H" a higher harmonic.

• SW100 - 100 MHz standing wave cavities. There are six of these cavities installed in the ring. Originally installed for ppbar operation, they are now used to capture the long lepton bunches at 3.5GeV/c and accelerate them at the beginning of the ramp.

• SW200 - 200 MHz standing wave cavities. These cavities provide lepton acceleration at intermediate energy ranges. Originally 32 cavities were installed in 4 groups of 8 cavities. There are now 20 left in the machine in 2 groups of 7 cavities and 1 of 6.

• TW200 - 200 MHz travelling wave cavities. These cavities provide acceleration for the proton and ion beams. There are four cavities installed, two 4-section cavities and two 5-section cavities. The two types are treated separately in the table.

• SC352 - 352 MHz superconducting cavities. These 4 cavities in 2 bimodules provide acceleration for the lepton beam at high energy. The cavities are damped by RF feedback in the presence of the high intensity proton beam. They can also be passively damped if necessary.

• SC400 - 400 MHz superconducting cavity for testing RF gymnastics with LHC beams in the SPS. During physics operation the cavity is passively damped.

• TW800 - Two of these 800 MHz travelling wave cavities are installed in the SPS. Their original purpose was to help stabilise the high intensity proton beam by adding extra sytnchrotron frequency spread, i.e. Landau damping. They have also been used for stochastic extraction experiments, more recently for echo experiments and will possibly be used for controlled blow-up of the proton beam for LHC in the future.

3) The R_{sh}/Q of the cavity. For the SW cavities this is the standard definition. In the case of the TW structures this is $L \times R_1/(2Q)$, where R_1/Q measured in Ω/m is given in Refs. [7] [16]. L is the length of the structure. The factor 2 comes from the different definitions of R_{sh}/Q in Linac terminology and the more usual equivalent circuit representation.

4), 5) The Q of the cavity. The higher order mode, HOM, resonances given are passively damped. In the case of the fundamental mode there is, in general, some means of changing the damping. The undamped Q, i.e no damping "n", is the Q with all HOM mode dampers, main coupling loop etc. attached. Passive damping, "p", is obtained by loading the cavity with an external resistor coupled to the cavity. Active damping, "a", is obtained with RF feedback. In the case of the 352MHz superconducting cavities two values are given for the actively damped Q. The first is with RF feedback alone, the second is with the single turn feedback loop added.

6) Shunt Impedance, R_{sh} , of one cavity. For the SW cavities this is $R_{sh}/Q \times Q$. For the travelling wave cavities in travelling wave mode this is $R_2 \times L^2/8$ where R_2 is the series impedance. For these cavities in standing wave mode, i.e unterminated at the ends, it is $R_1 \times L/4$.

7) Number of cavities, N, as installed in 1996.

8) Total $R_{sh}/Q = N \times R_{sh}/Q$.

9) Total $R_{sh} = N \times R_{sh}$. Note that these figures are given for each Q value assuming each cavity is damped in the same way. In practice this may not be the case. For example the leptons are captured using three 100MHz cavities with active damping, the other three being passively damped. This is the situation throughout the supercycle.

10) References providing the information.

Table 3 gives other resonances that are known to exist in the cavities but whose impedance is unknown. These have been found by observation using the beam or by measurement in the laboratory.

The resonances with known impedance are displayed visually in Fig.1.

2.2 Kickers and Septa

Measurements with the beam, [1], showed that there is a significant source of impedance around 400MHz which cannot be attributed to the RF cavities. The impedance indicated covers a range of more than 100 MHz and consists of several resonant peaks within this bandwidth. The low centre frequency suggested a fairly large object with radius around 35 cm as the source. A search around the ring and discussions with colleagues, [17],[18],[19], led to the identification of the magnetic septa MSE used for extraction as a likely candidate. Calculations with ABCI [20] using a simplified septum geometry gave good agreement with the frequencies observed and this was confirmed by measurements in the laboratory on a spare element. Fig.2 shows the real part of the impedance as calculated by ABCI and Fig.3 gives an example of the laboratory measurements. The R_{sh}/Q values have not been measured yet. Due to its length and lack of azimuthal symmetry the structure is not suited for modelling with existing codes. Simple estimations suggest that the R_{sh}/Q can be high but the transit time factor is difficult to estimate because of the large beam pipe connections. It is proposed to try and measure the R_{sh}/Q in the laboratory using the standard techniques. If our suspicions concerning this source are confirmed it will be necessary to shield the circulating beam from the tank as has already been done for LEP septa. The first part of Table 4 gives the present knowledge concerning these elements. Note that there are already 16 of these devices in the machine and a further 8 will be installed for the LHC beam extraction.

The second part of the Table gives other possible sources in this frequency range. These are the injection kicker elements, the collimators and the electrostatic septa. In these devices the circulating beam is contained within a narrow chamber except at the entry and exit points where there is a gap and where it can see the external tank. This can be a more dangerous situation in that the transit time factor may be significantly increased. Measurements are necessary to check this.

2.3 Pumping ports

Beside each bending magnet there is an ensemble consisting of a pumping port plus bellows. This ensemble is attached to the vacuum chamber, of smaller dimensions on each side forming a cavity. Estimations of the impedance of these elements were made even before the building of the SPS [22] and damping resistors were installed to combat coupled bunch instabilities. The contribution of these elements to the low frequency inductive machine impedance has also been investigated and shown to be dominant [23]. The importance of the high frequency resonant structure has more recently been shown in measurements with single bunches [1]. The associated shunt impedances for a more realistic geometry than used in the original estimations, have been estimated using different computer codes [24]. It is the large number of these elements that makes their contribution to the impedance so important. The four main types of geometry are shown in Fig.4. There are 782 of the first type which is by far the most prevalent, however the other three geometries exist in significant numbers, of the order of 100 all together. For the dominant geometry, see Fig.5 the ABCI output is given in Fig.6. The frequencies calculated agree extremely well with measurements observed on the beam. Our measurements in the laboratory give the quality factors to be ~ 70. Beam measurements [25] suggest a lower limit of ~ 20. The final results are summarised in Table 5. In this table the frequencies are taken from the ABCI calculation and the R_{sh}/Q values are the values taken from [24] which were calculated for a slightly different geometry.

3 Transverse Plane

Similar data to that already presented for the longitudinal modes in Table 1 is given for the transverse modes in Table 6. The definitions of resonant frequency, source, quality factor and the reference from which the data can be found is as before.

The $R_\perp/Q$ is the standard definition for the SW cavities. For the travelling wave cavities, the value quoted is $R_1/\ldots$ and is in Ω/m.

The transverse impedance, $Z_\perp$ is defined by $R_\perp/Q \times Q \times 2\pi f_{res}/c$ for the standing wave cavities and is given for the total number of cavities. c is the velocity of light, For each travelling wave cavity it is given by $Z_\perp = R_1/Q \times Q \times L/4 \times 2\pi f_{res}/c$, where the factor 4 is half from the definition of R/Q and half from the SW use of the cavity.

4 Conclusions

We have presented here the data that we have for the resonant impedances in the SPS ring. Our knowledge is not complete particularly concerning the septa contribution where further measurements need to be done in the laboratory. Updates will be issued as new information becomes available.

Acknowledgements

A large number of people have been consulted in the endeavour to unravel the impedance structure of the SPS. Their names can be found in the reference section. We thank them all very much for their patience.

References

[1] T.Bohl, T.Linnecar, E.Shaposhnikova, Measurement of the longitudinal SPS impedance up to 3GHz. SL-MD Note 211, July 2, 1996

[2] D.Boussard. Private communication.

[3] G.Lambert, Mise en service de la contre-réaction haute fréquence sur une cavité à modes stationnaires à 100MHz, SL/RFS/Note 90-4, 1990

[4] D.Boussard, P.Baudrenghien, T.Linnecar, G.Rogner, W.Sinclair, The 100MHz RF system for the CERN collider, CERN SPS/88-27(ARF) and EPAC '88 Rome, 1988

[5] P.E.Faugeras, H.Beger, H.P.Kindermann, V.Rödel, G.Rogner, A.Warman, The new RF system for Lepton Acceleration in the CERN SPS, CERN SPS/87-19 (ARF) and PAC '87 Washington, 1987

[6] F.Caspers, G.Dôme, H.P.Kindermann, A new type of broadband, higher mode coupler using parallel ridged waveguide in comparison with a coaxial filter version, CERN SPS/87-23 (ARF) and PAC '87 Washington, 1987

[7] G. Dôme, The SPS Acceleration System Travelling Wave Drift-Tube Structure for the CERN SPS, CERN-SPS/ARF/77-11, 1977

[8] G.Rogner, Private communication

[9] D.Boussard, G.Lambert, T.P.R.Linnecar, Improved Impedance Reduction in the CERN SPS Superconducting Cavities for High Intensity Proton Operation, PAC '93 Washington, 1993

[10] E.Montesinos, Private communication

[11] V.Rödel, Private communication

[12] P.Baudrenghien, Private communication

[13] G.Dôme, Private communication

[14] E.Haebel, Couplers, Tutorial and Update, Particle Accelerators, Vol.40, p141-159, 1990

[15] E.Haebel, P.Marchand, J.Tückmantel, An Improved Superconducting Cavity Design for LEP, CERN/EF/RF 84-2, 1984

[16] G.Dôme, W.Schminke, The Slotted Iris Structure, SPS/ARF/Technical Note/WS/gs/81-41, 1981

[17] B.Goddard, Private communication.

[18] G.Schröder, Private communication.

[19] L.Vos, Private communication.

[20] Y.Chin, User's Guide for ABCI Version 8.7, CERN SL/94-02 (AP), 1994

[21] D.Boussard, V.Rödel, Status of the LHC prototype superconducting RF cavity, SL/Note 93-90 (RFS), 1993

[22] G.Dôme, Longitudinal coupling impedance of cavities for a relativistic beam, CERN LABII/RF/Note/73-2, 1973

[23] L.Vos, Computer calculation of the longitudinal impedance of cylindrical symmetric structures and its application to the SPS, CERN SPS/86-21 (MS), 1986

[24] W.Höfle, Calculation of longitudinal modes in the SPS inter-magnet pumping ports, CERN SL/Note 96-40 (RF), 1996

[25] T.Bohl, T.P.R.Linnecar, E.Shaposhnikova, Measuring the Resonance Structure of Accelerator Impedance with Single Bunches, CERN-SL-96-62 RF, 1996

n	f_{res} MHz	Source	R_{sh}/Q Ω	Q (approx.) meas. or calc.	Damp. type	R_{sh} 1 cav. kΩ	No. cav.	R_{sh}/Q total kΩ	R_{sh} total kΩ	Ref.
1	100.0	SW100-F	230	150	p	34.5	6	1.380	207	[2]
				3400	a	782			4692	[3]
				34000	n	7820			46920	[4]
2	200.2	TW200-F	6284	150	n	1430	2	12.57	2860	[7]
			5029	120	n	920	2	10.06	1840	[7]
3	200.4	SW200-F	186	80	p	14.9	20	3.720	298	[5]
				40000	n	7440			148800	[6]
4	288.0	SW100-H1	24.6	490	p	12	6	0.148	72	[4], [8]
5	306.0	SW200-H1	16	4400	p	70.4	20	0.320	1408	[6]
6	352.0	SC352-F	232	2000	a	486	4	0.928	1944	[9]
				667	a	162			648	[10]
				500	p	116			464	[10]
				3E7	n	7E6			28E6	[9]
7	400.0	SC400-F	44.5	666	p	30	1	0.045	30	[11]
8	405.4	SW100-H	7	596	p	4.17	6	0.043	25	[12]
9	446.0	SW200-H	8	1200	p	9.6	20	0.160	192	[6]
10	540.0		7	690	p	4.8	20	0.140	97	
11	548.2	SW100-H	13.5	9500	p	128.3	6	0.081	770	[12]
12	551.0		13.5	11000	p	148.5	6	0.081	891	
13	599.0	SW200-H	14	x10 1500	p	21	20	0.284	420	[6]
14	629.0	TW200-H	432	500	p	108	2	0.864	216	[13]
			346	500	p	86	2	0.693	172	
15	637.0	SC352-H	24	4000	p	96	4	0.096	384	[14], [15]
16	639.0		54	7000?	p	378	4	0.216	1512?	
17	784.0	SC400-H	1.6	40000	p	64	1	0.002	64	[11]
18	790.0		1	40000	p	40	1	0.001	40	
19	799.0	SW200-H	13	1000	p	13	20	0.260	260	[6]
20	800.8	TW800-F	3227	150	n	968	2	6.454	1936	[16]
21	895.0	SC400-H	8.9	40000?	p	356	1	0.009	356	[11]
22	984.0	SW200-H	6	9900	p	59.4	20	0.120	1188	[6]
23	1006.0	SC352-H	25.5	3000	p	76.5	4	0.102	306	[14]
24	1076.0	SC400-H	4.4	40000?	p	176	1	0.004	176	[11]
25	1109.0	SC400-H	2.2	40000?	p	88	1	0.002	88	[11]

Table 1: RF cavity resonances, known impedances

NB. 486 MHz (SWC100, 1 undamped).

Cavity type / Year	TW200 4 section	TW200 5 section	TW800	SW100	SW200	SC352	SC400
1976	2						
1977	2						
1978		3					
1979	3	1					
1980	2	2	1 2/Aug				
1981 to 1986	2	2	2				
1987	2	2	2	4	8	1	
1988	2	2	2	6	24	1	
1989	2	2	2	6	32	1	
1990	2	2	2	6	32	2	
1991	2	2	2	6	32	1	
1992	2	2	2	6	24 28/May	3 2/Aug	
1993	2	2	2	6	28	2	
1994	2	2	2	6	21	4	
1995	2	2	2	6	21	4	1
1996	2	2	2	6	20	4	1
2001	2	2	2				4?

Table 2: Cavities in the SPS, (changes in january each year).

n	f_{res} MHz	Source	No. cav.	Ref.
1	912	TW200-H	4	[16]
2	978	TW200-H	4	[16]
3	1075	TW200-H	4	meas
4	1130	TW200-H	4	meas
5	1284-1328	TW200-H	4	meas
6	1334-1364	TW200-H	4	meas
7	1395	TW200-H	4	meas
8	1445	TW200-H	4	meas
9	1503	TW200-H	4	meas
10	1860	TW800-H	2	[16]
11	1910	TW800-H	2	[16]
12	2500	TW800-H	2	[16]
13	2780	TW800-H	2	[16]

Table 3: RF cavity resonances, only frequencies are known

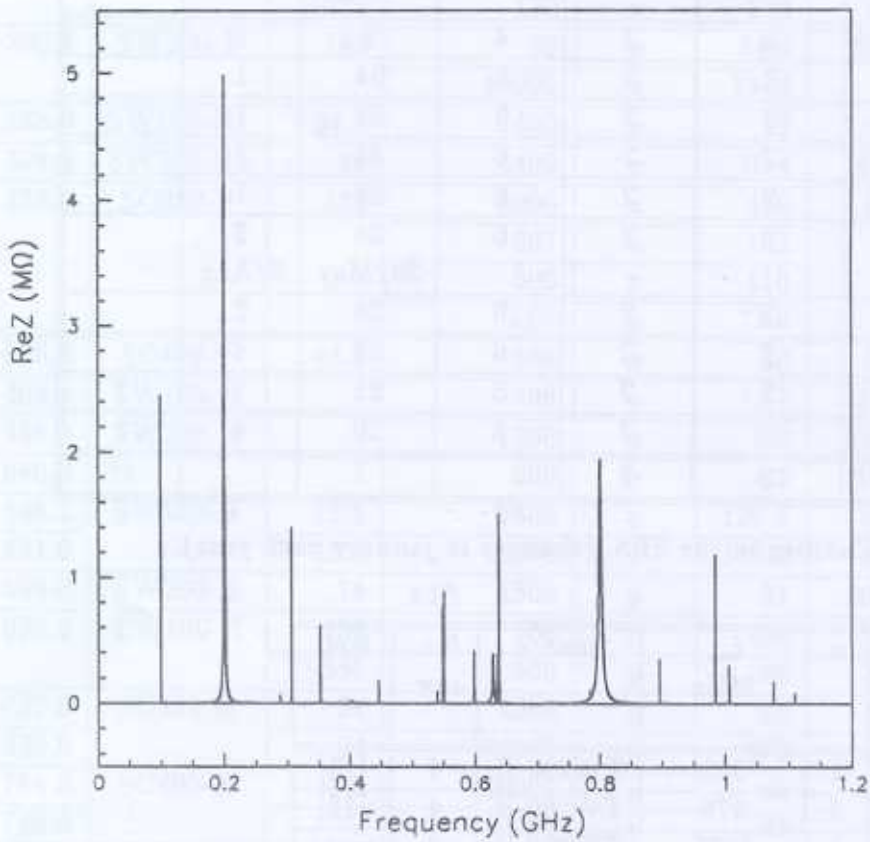

Figure 1: Real part of the impedance of the RF cavity resonances.

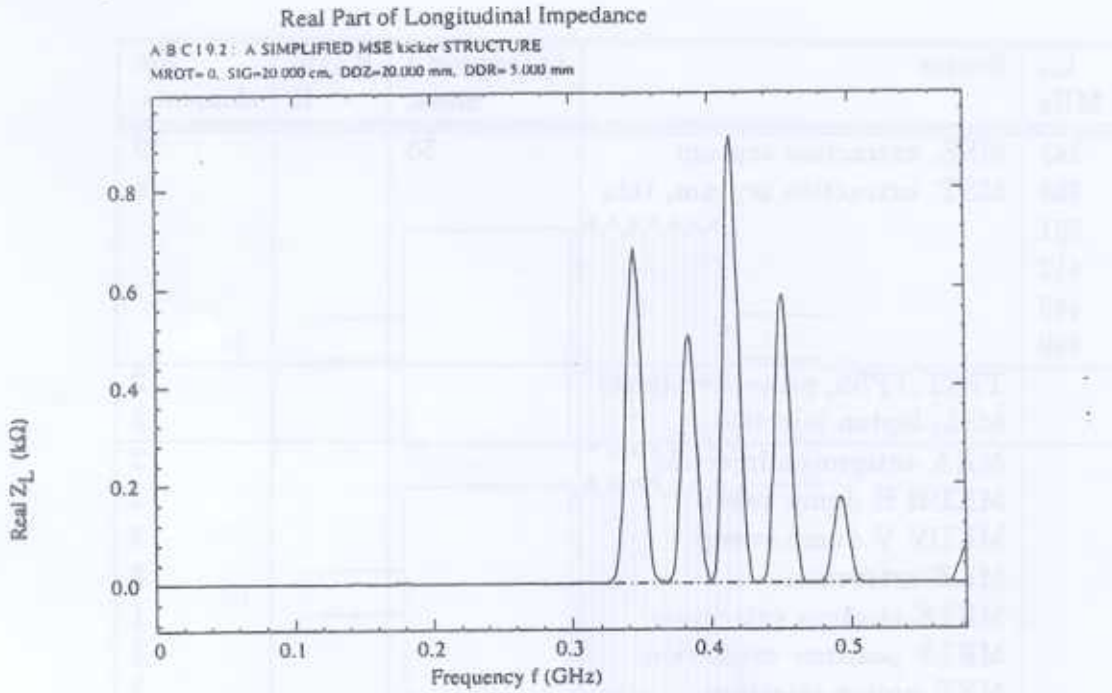

Figure 2: Real part of the impedance for a simplified geometry of the MSE septum magnet in the SPS obtained with ABCI

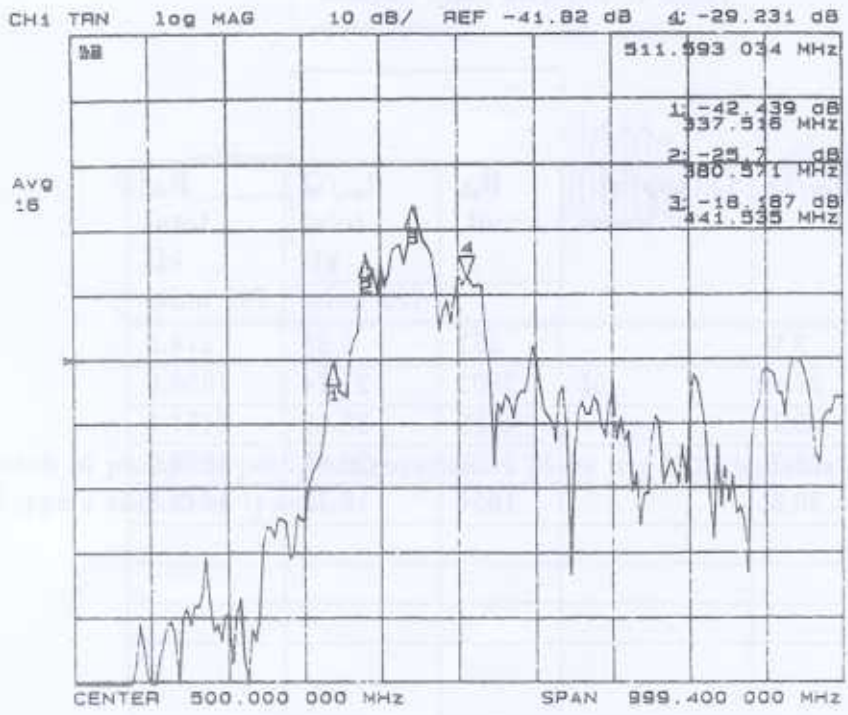

Figure 3: Laboratory measurement of the resonant frequencies of the MSE. With the excitation used both longitudinal and transverse resonances may be seen.

n	f_{res} MHz	Source	Q (approx.) meas.	R_{sh}/Q Ω	No. elements.
1	343	MSE, extraction septum	50		10
	358	MST, extraction septum, thin			6
	381				
	412				
	449				
	490				
2		TPST,TPSS, protective shield			2
		MSL, lepton injection			2
3		MKA antiproton injection			2
		MKDH H dump sweep			3
		MKDV V dump sweep			2
		MKE extraction			3
		MKLE electron extraction			1
		MKLP positron extraction			1
		MKP proton injection			3
		MKQH H q meas.			1
		MKQV V q meas.			1
4		ZS electrostatic septum			10
		TCE extraction collimator			2

Table 4: 400MHz band sources

n	f_{res} MHz	R_{sh}/Q	Q (approx.) meas.	R_{sh} 1 unit. Ω	R_{sh}/Q total kΩ 782 units	R_{sh} total kΩ 782 units
1	1.39	3.9		351	3.05	274.5
2	1.55	27.8	55	2502	21.74	1956.6
3	1.91	45.1		4059	35.27	3174.1
4	2.40	26.7		2403	20.88	1879.2
5	2.96	20.6		1854	16.11	1449.8
6	3.16					
7	3.44					
8	3.59					
9	3.78					
10	4.23					

Table 5: Impedances introduced by pumping ports

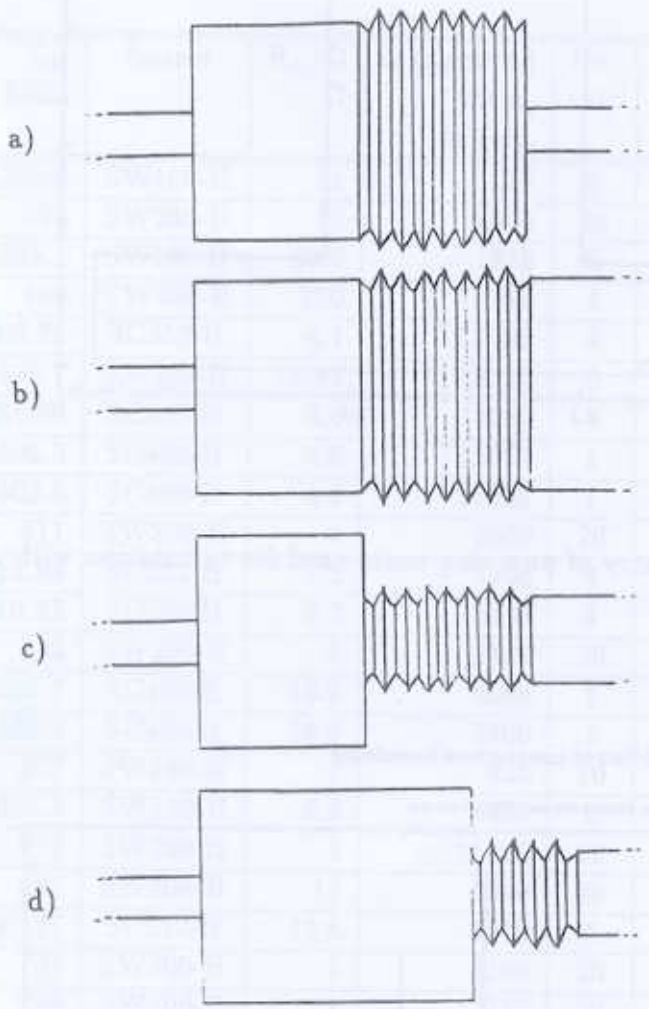

Figure 4: Sketch of pumping port configurations. There are 782 elements of type a, 46 of type b, 56 of type c and 13 of type d.

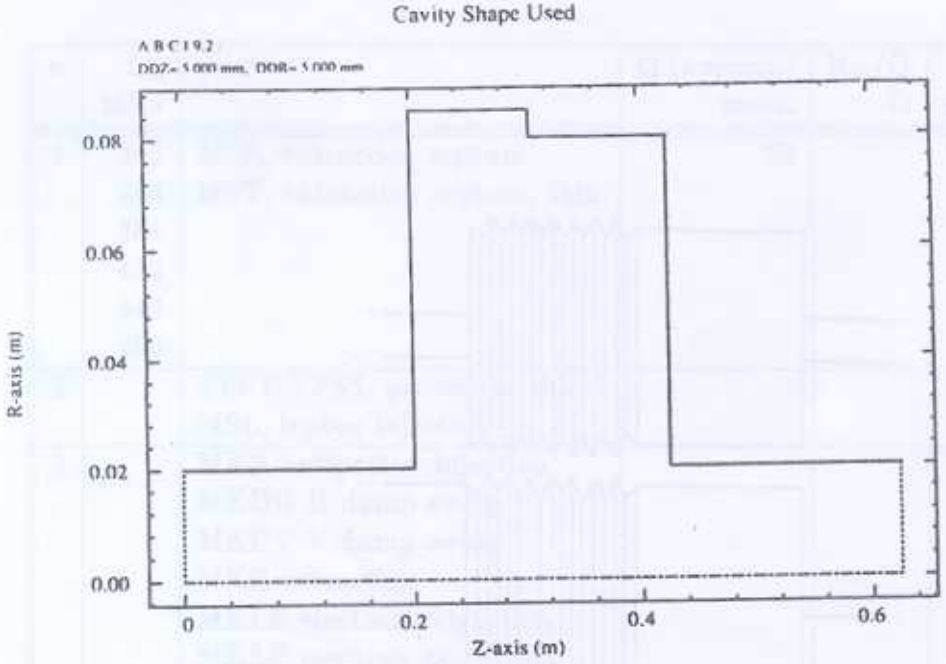

Figure 5: Simplified geometry of pumping ports used for calculation with ABCI

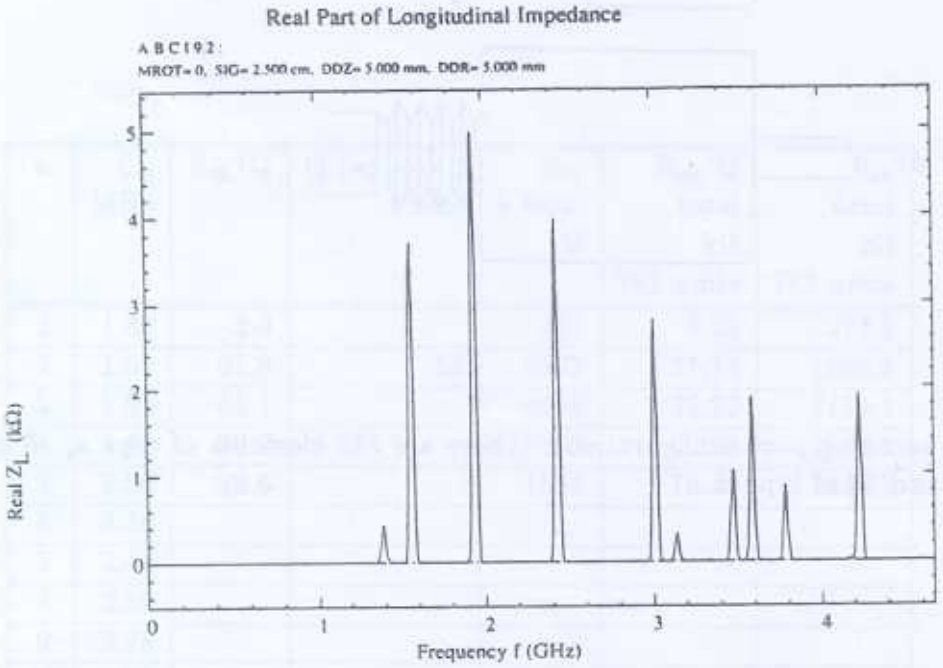

Figure 6: Real part of the impedance for the pumping ports as given by ABCI

n	f_{res} MHz	Source	$R_\perp/Q$ Ω	Q (approx.) meas. or calc.	No. cav.	$Z_\perp$ total MΩ/m	Ref.
1	285.8	SW100-H	21	177	6	1.32	[12]
2	395	SW200-H	18	1500	20	4.47	[6]
3	395.1	SW100-H	30.3	1880	6	2.83	[12]
4	460	TW200-H	250	838	4	37.3 H	[13]
5	466.75	SC352-H	4.1	17000	4	2.73	[14]
6	476.7	SW100-H	14.83	13000	6	11.55	[12]
7	481.99	SC352-H	3.6	14000	4	2.04	[14]
8	500.5	SC400-H	4.9	12000	1	0.616	[21]
9	502.6	SC400-H	4.3	12000	1	0.543	[21]
10	511	SW200-H	3	2500	20	1.61	[6]
11	511.94	SC352-H	5.5	5600	4	1.32	[14]
12	519.42	SC352-H	3.7	5700	4	0.92	[14]
13	522	SW200-H	6	2100	20	2.75	[6]
14	536.7	SC400-H	16.1	2500	1	0.452	[21]
15	538.2	SC400-H	16.9	2500	1	0.476	[21]
16	577	SW200-H	7	820	20	1.39	[6]
17	631.3	SW100-H	9.2	4400	6	3.21	[12]
18	677	SW200-H	3	12400	20	11.06	[6]
19	681	SW200-H	13	2000	20	7.42	[6]
20	697.27	SC352-H	12.8	1000	4	0.75	[14]
21	707	SW200-H	1	3100	20	0.92	[6]
22	759	SW200-H	1	780	20	0.25	[6]
23	791.67	SC352-H	1	1000	4	0.07	[14]
24	938.5	TW200-H	16.4	1500	4	2.49 V	[13]
25	1146	TW800-H	335	1000	2	4.0	[16]
26	2210	TW800-H			2		[16]
27	2350	TW800-H			2		[16]

Table 6: Transverse modes in the RF cavities